Pion absorption mechanism for very light nuclei

Hitoshi Yokota
Department of Physics, Tokyo Institute of Technology, Ohokayama, Meguro-ku, Tokyo 152, Japan
(Received 29 September 1992)

Double- and triple-coincidence data for pion absorption on ^{3}He and ^{4}He are analyzed using a multistep reaction model with Monte Carlo calculations. The cross sections far from the two-nucleon absorption region could be reproduced very well using only well-known reaction mechanisms and nuclear data. Clear evidence for the two-step process is also shown.

PACS number(s): 25.80.Ls, 25.10.+s

Since early 1980s pion absorption studies have been focused on the problem of the discrepancy between total absorption cross section and direct two-nucleon absorption (2NA) cross sections associated with the fundamental reaction $\pi^+ d \rightarrow p + p$, and a large amount of data have been accumulated during the past decade on total absorption cross section, the angular distribution of inclusive single-arm cross section, and the angular correlations between two or three energetic emitted particles. In order to explain the discrepancy, contributions from fundamental processes other than the $\pi^+ d \rightarrow p + p$ reaction have been examined especially for the (π,pn) and (π,Nd) reactions, and other complex processes. The ratios of the direct (π^+,pp) cross section to the direct (π,pn) cross section were about 15 or ^{3}He [1,2], 20 for ^{4}He [3], and smaller for ^{6,7}Li [4]. The ratio depends on incident pion energy as well as on target mass, however, the contribution of the (π,pn) process is at most 20% of that of the (π^+,pp) process. The total cross sections of the direct (π,Nd) reaction are also small and about 1.5 mb for ^{4}He [3] and 1 mb for ^{6,7}Li [5]. Therefore, these processes are not sufficient to explain the discrepancy.

Two rather extreme models have been considered and applied to describe the double- and triple-coincidence data. One is the two-nucleon absorption (2NA) with strong initial- and final-state interactions. The other is the quasifree two- and many-nucleon absorption with a long mean free path for emitted particles. We refer hereafter to the former as the short mean-free-path model (SMFP), and to the latter as the many-body absorption (MBAB) model. Calculations for these models have been performed using Monte Carlo (MC) simulations, because the absorption reaction involves many reaction steps and reaction channels, and the detectors used have generally large solid angles. Quantum dynamical studies on this reaction have been done only on limited conditions; for example, a calculation from the pion-nucleus optical potential [6], a macroscopic pion transport calculation [7], and a nucleon rescattering calculation up to the second order for the three-nucleon system [8]. Therefore, at present, the Monte Carlo calculation which includes both pion and nucleon rescattering processes seems more appropriate for the description of the complex process, if the interference between channels to the same final state is not significant at the incident pion energy of around 100 MeV.

A typical code of the SMFP model is well known as the intranuclear cascade (INC) code [9], where the mean free path is deduced from the cross section of the corresponding free reaction with the correction for the Pauli blocking effect. The mean free path for pion absorption in nuclei is extracted from empirical data of total absorption cross section on rather light nuclei. The predictions of the INC calculation reproduces fairly well the total absorption cross section, the single-arm data, and the two-nucleon coincidence cross sections for light nuclei. The angular distributions of the (π^+,p) and direct (π^+,pp) cross sections are similar to that of the free $\pi^+ + d \rightarrow p + p$ reaction, and they could be well reproduced by the INC calculation. The angular correlation of the (π^-,pp) cross section showed two broad peaks [10]. One is the 90° correlation owing to the hard final-state interaction (FSI) between the emitted nucleon from the two-nucleon absorption and a spectator nucleon. The other is the 180° correlation due to the 2NA by an energy-degraded pion through initial-state interactions (ISI). They could be well reproduced by the INC calculation. On the other hand, the INC predictions for the direct 2NA cross sections are larger than the experimental value by factors of 1.3 for Li, 2.2 for C, and larger for heavier nuclei [11]. The reason for this discrepancy is probably due to the simplified nuclear distribution function applied to the INC code, especially at the nuclear surface.

The MBAB model was originally introduced to explain the rapidity distribution of emitted nucleons following pion absorption and the missing cross section. Therefore, the contribution of the MBAB process is expected to be as large as or much larger than that of the two-nucleon process. Recently, elaborate studies were performed for ^{3}He and ^{4}He by Backenstoss *et al.* [12–14] at counter configurations which favor three-nucleon or four-nucleon phase space. They found that the angular distribution of the ^{3}He(π^+,pp) cross section and the energy spectrum of coincident protons were very well reproduced by the MBAB model. The broad component of the ^{3}He(π^+,pp) angular distribution is very similar to the three-body phase space. It might contain large amount of contribu-

tions from a genuine three-nucleon absorption (3NA) process, because the matrix element for the process is considered to be constant throughout the whole phase space. Triple-coincidence data of pion absorption on ^{4}He also showed the existence of a 3NA component. Differential cross section as a function of the momentum of the undetected nucleon could be reproduced very well by a Monte Carlo simulation weighting the four-body phase space using the nucleon momentum distribution from the $(e,e'p)$ data.

The purpose of this paper is to test how far the ^{3}He and ^{4}He data can be explained by the SMFP model. This work will help to estimate the fraction of contributions from various possible processes. The INC code used for heavier target is not appropriate for very light nuclei. Therefore, we developed a Monte Carlo code which treats up to second steps of the absorption reaction.

A pion absorption model with an optical potential was studied by Masutani and Yazaki [6], assuming that the imaginary part of the potential consists of quasifree and absorption terms. In this model, the reaction cross section can be divided into two terms

$$\sigma_r=\sigma_{\rm qf}^{(0)}+\sigma_{\rm abs}^{(0)} .$$

$\sigma_{\rm qf}^{(0)}$ ($\sigma_{\rm abs}^{(0)}$) is the cross section for which the first nonelastic interaction is the quasifree process (true absorption). As the scattered pion may be absorbed on the second interaction, $\sigma_{\rm qf}^{(0)}$ can be divided into three terms

$$\sigma_{\rm qf}^{(0)}=\sigma_{\rm esc}^{(1)}+\sigma_{\rm qf}^{(1)}+\sigma_{\rm abs}^{(1)} .$$

Repeating the process, the total absorption and quasifree cross sections corresponding to the experimental observable are given by

$$\sigma_{\rm abs}=\sigma_{\rm abs}^{(0)}+\sigma_{\rm abs}^{(1)}+\cdots ,$$
$$\sigma_{\rm qf}=\sigma_{\rm esc}^{(1)}+\sigma_{\rm esc}^{(2)}+\cdots .$$

Exact division of $\sigma_{\rm qf}^{(0)}$ is not simple. In the present calculation, a semiclassical model was applied. The approximation is not reliable on absolute cross sections; however, for the reactions concerned, momentum transfers are larger than 250 MeV/c at each step and the quasifree limit defined by Goldberger and Watson [15] is satisfied. This model can also reasonably treat the angular dependence of scattered and recoiled particles.

For very light nuclei $\sigma_{\rm abs}^{(0)}$ can be estimated from the direct (π,pp) data after correcting for the attenuation of scattered pions through absorption processes. These attenuation effects can be evaluated by the attenuation model introduced by Rogers and Saylor [16]. The transmission probability for the outgoing particle p_i is given by

$$T_i=\int \psi^*(r_{is})T_{is}(\sigma_{is},r_{is})\psi(r_{is})dr_{is} ,$$

where $\psi(r_{is})$ is the relative bound state wave function of p_i and the spectator nucleus s, and σ_{is} the total scattering cross section of p_i on s. The transmission coefficient T_{is} used is what was adopted by Haracz and Lim [17]

$$T_{is}=\begin{cases}\{1+[1-\sigma_{is}/(4\pi r_{is}^2)]^{1/2}\}/2 & \text{for } r_{is}\geq\sqrt{\sigma_{is}/4\pi}\\ 0 & \text{for } r_{is}<\sqrt{\sigma_{is}/4\pi} .\end{cases}$$

This coefficient could well reproduce the attenuation parameters of the $(p,2p)$ reaction for ^{2}H, ^{3}He, and ^{4}He in wide energy ranges of incident protons. A typical value of T_i for a proton from the ^{3}He (π^+,pp) reaction is 0.87, using an Irving-Gun function for ^{3}He.

$\sigma_{\rm abs}^{(0)}$ can be obtained from $\sigma_{\rm dir}(2N)$, the direct ^{3,4}He(π^+,pp) data, and attenuation parameters T_1 and T_2

$$\sigma_{\rm abs}^{(0)}=\sigma_{\rm dir}(2N)/T_1T_2 ,$$

then the cross section for the FSI process in Fig. 2 is

$$\sigma_{\rm FSI}=\sigma_{\rm abs}^{(0)}-\sigma_{\rm dir}(2N) .$$

$\sigma_{\rm qf}^{(0)}$ may be considered very near to the (π,π') data, and $\sigma_{\rm abs}^{(1)}$ is obtained from $T_{\rm abs}$, the transmission probability of scattered pions through pion absorption on the spectator nucleus,

$$\sigma_{\rm abs}^{(1)}=(1-T_{\rm abs})\sigma_{\rm qf}^{(0)} .$$

In the Monte Carlo calculation relativistic kinematics calculations were performed at all stages. Each step is assumed to proceed in on-energy-shell interaction, and the momentum distribution function of nucleon and clusters in He were taken from the $(e,e'p)$ and $(e,e'd)$ data [18,19]. Three types of events were created in proportion to the cross sections, $\sigma_{\rm FSI}$, $\sigma_{\rm abs}^{(1)}$, and $\sigma_{\rm dir}(2N)$, and numbers of coincident event were accumulated for the experimental detector arrangements.

Angular distribution of the coincident proton yield was observed [12] for ^{3}He with an E counter fixed at 117° for particle 1 at the incident pion energy of 120 MeV, and is shown in Fig. 1 as a function of the angle of counter 2. A narrow peak at around $\theta_2=40°$ is attributed to the quasifree 2NA on a pn pair and is superimposed on a small and broad component. The shape of the narrow peak

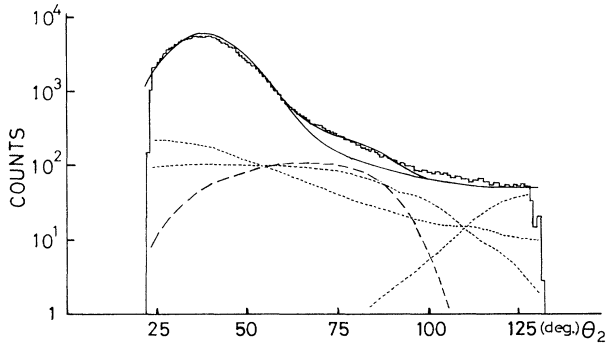

FIG. 1. Angular correlation of the reaction ^{3}He(π^+,pp) at $T_\pi=120$ MeV and $\theta_1=117°$. Solid lines: sum of MC calculations for one- and two-step processes, with ISI (upper) and without ISI (lower). Dotted lines: MC calculations for two-step processes with hard FSI, three lines correspond to particle interchange processes. Dashed line: for two-step process with ISI. Data are taken from Ref. [12].

should be reproduced by the Fermi momentum of the absorbing *pn* pair. The angular resolution of the counter 1 was as large as $\pm 14°$, then the peak must be significantly broadened. As we can see in Fig. 1, the shape of the peak can be well reproduced by the present MC calculation of the SMFP model in an angular range from 25° to 60°. In this model, the broad component is dominated by the contributions from the Feynman graph (a) in Fig. 2. A dotted line which is flat at small angles indicates the MC results for the graph (a), where one of two emitted particles from the primary 2NA process is detected by the counter 1 and the other is scattered into the counter 2 through the hard FSI with spectator nucleon. Another dotted line decreasing gradually with angle is for the particle interchange process, where the direct proton from pion absorption is detected by the counter 2 and the scattered proton by counter 1. At a large angle of θ_2, the opening angle between the two counters approaches 90°, and contributions from the process where two protons in the FSI are detected by the two counters increase sharply at angles larger than $\theta_2 = 100°$, as we can see from the dotted line in Fig. 1. The summed yield for the graph (a) have a very similar angular distribution to that of the three-body-phase-space simulation [12].

Gross shape of the experimental angular distribution seems to be reproduced by the direct 2NA and the proton-proton FSI, as indicated by a lower solid line; however, significant discrepancy from the data can be seen in an angular range between 65° and 85°. This situation is similar for the MBAB model. The angular range corresponds to the opening angle of 180° between the two counters. As we discussed in Ref. 10, the ISI of incident pions with target nucleon before absorption contributes to the 180° correlation. The dashed line shows the yields for the Feynman graph (b) in Fig. 2. It fills the missing part almost completely, and the summed yield shown by the upper solid line reproduces the data very well.

The proton energy spectra for the ^{3}He(π^+,*pp*) reaction at 120 MeV were also measured [13] with a total-absorbing plastic-scintillator hodoscope and a long position-sensitive time-of-flight (TOF) counter. Two counter configurations were chosen. One was for the direct 2NA: 117° for the *E* counter and −40° for the TOF counter. The other was 117° and −90°, where 2NA is strongly suppressed and the contributions from nonlocalized phase-space processes might become observable. The proton energy spectrum of the coincidence events in the *E* counter is shown in Fig. 3, for the counter configuration of 117° and −90°. It has a broad peak at about 75 MeV, a small shoulder at 110 MeV, and a rather enhanced tail at the low-energy side of the peak. The gross shape of the whole spectrum was well fitted by the three-particle phase-space distribution.

For the SMFP model, two-step processes of the Feynman graph (a) and (b) will contribute equally to the spectrum through hard FSI and ISI. Coincidence yields from two-step processes are sensitive to the counter configuration. As detailed description is not given in Ref. 13, we consulted Ref. 3, where both the *E* counter and TOF counter have wide angular acceptance. The MC results are given in Fig. 3 by dotted lines for the graph (a) and a dashed line for the graph (b). The dash-dotted line is the contribution from the spectator emission process, Fig. 2(c). The summed energy spectrum has a broad peak at 85 MeV, a shoulder due to the ISI at 110 MeV, and a small enhancement at low energy. The shoulder at 110 MeV can be well reproduced by the ISI, as we can see in Fig. 3. The energy of the broad peak is shifted to lower energy by 10 MeV from the energy of protons emitted directly through the 2NA process. This value is not far from the experimental result of 15 MeV (Fig. 2 of Ref. [13]), although the peak energies are shifted to higher energy in comparison with the data. The spectator emission process is not sufficient to explain the enhanced low-energy proton yields. The argument on the mass of the exchanged particle was also given in Ref. [13] about a Feynman graph for a mechanism involving three nucleons. In the present MC calculation, various reaction processes are important and the differential cross section as a function of the exchange mass cannot show a clear peak.

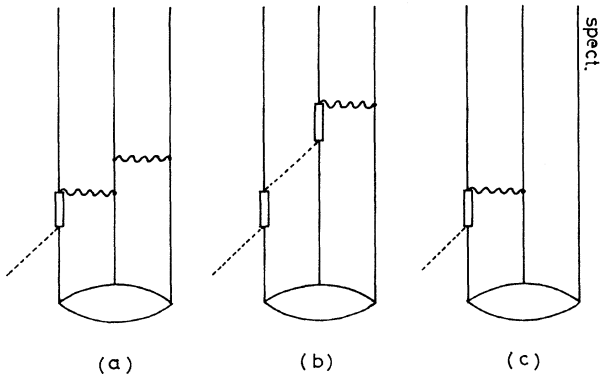

FIG. 2. Feynman graphs for (a) two-step process with FSI, (b) two-step process with ISI, and (c) the spectator emission process.

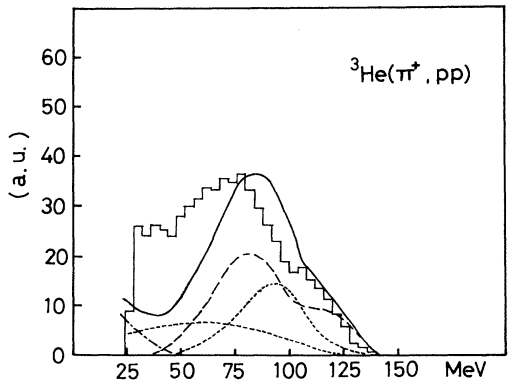

FIG. 3. Coincident proton energy spectrum at $\theta_1 = 117°$ and $T_\pi = 120$ MeV, for the counter configuration of $\theta_1 = 117°$ and $\theta_2 = -90°$. Solid line: sum of MC calculations. Dotted lines: for two-step processes with hard FSI. Dashed line: for two-step process with ISI. Dash-dotted line: for the spectator emission process. Data are taken from Ref. [13].

Three-nucleon emission cross sections from pion absorption in ^{4}He were measured at the Paul Scherrer Institute (PSI) [14] and TRIUMF [20]. Triple coincidence measurements will make it possible to follow the behavior of the fourth nucleon and to reveal the existence of a three-nucleon component in the four-nucleon channel and a four-nucleon phase-space-like contribution. The counter configuration for PSI consisted of a total absorption scintillator hodoscope and two TOF detectors for neutrons and charged particles. They had large solid angles and were arranged in a reaction plane at 72°, 240°, and 305°. The opening angle between two TOF counters ranges from 32.6° to 97.4°. Then the counter arrangement is rather favored for the two-step processes with hard FSI. The counter configuration for TRIUMF was more suitable for the two-step processes, because the opening angles were about 95° at the center of counters between RA and RB counters defined in Ref. [20], and RA and TA counters. These counters also had large angular acceptance.

The MC calculation for the SMFP model was performed about the PSI data, because the absolute cross sections are given. The Feynman graphs for ^{4}He can be described by adding a spectator nucleon line to the graphs in Fig. 2. The direct 2NA cross section was taken from recent experimental results [3,21]. The MC results for the differential cross section as a function of the momentum of undetected neutron for ^{4}He(π^+,ppp)n are shown in Fig. 4. The dotted line represents the contributions from the two-step process with hard FSI, and the dashed line is for the ISI process. The effect of the spectator emission is small and is indicated by the dash-dotted line. The summed cross section reproduces the shape of the peak at around 100 MeV/c, which corresponds to the neutron momentum distribution in the target.

The two-step process can also estimate the ^{4}He(π^+,ppn)^{1}H cross section. The process with hard FSI

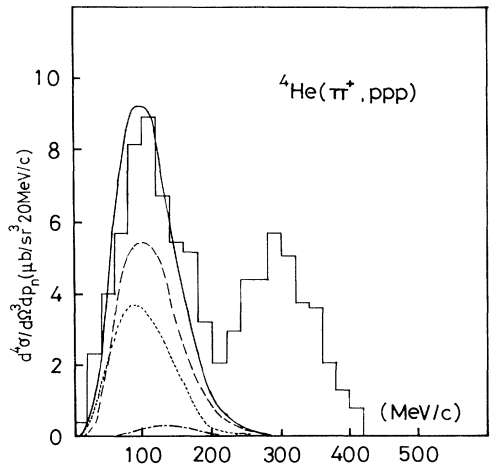

FIG. 4. Differential ^{4}He(π^+,ppp) cross section as a function of the undetected neutron momentum. The solid line represents the sum of MC calculations for two-step processes. Data are taken from Ref. [14].

favors the reaction, because the n-p scattering cross section is two times as large as the p-p cross section at around 100 MeV. On the contrary, the process with ISI is hindered due to the reaction: the $\pi^+ + n \rightarrow \pi^0 + p$ or $\pi^+ + nn \rightarrow p + n$ reaction. In effect, the SMFP model predicts almost as large a cross section as the reaction (π^+,ppp), and is a little smaller than the data.

The peak corresponding to higher-momentum spectator nucleon for ^{4}He(π^+,ppp) cannot be explained by the two-step processes in Fig. 2. However, if quasibound particle emission, such as the direct (π^+,pnp) process, has any contributions in an analogous process as the direct (π^+,pd) reaction observed for ^{4}He, ^{6,7}Li, and C, the momentum of undetected nucleon may have a peak at 300 MeV/c. For the ^{4}He(π^+,npp) cross section, the pion absorption process must be the reaction (π^+,ppp) or (π^+,ppn), then the ^{4}He(π^+,npp) cross section at 300 MeV/c should be much smaller than the ^{4}He(π^+,ppp) cross section in agreement with the experiment [14]. The ratio of cross section at 300 MeV/c to that at 100 MeV/c is hard to estimate for the SMFP model, because the direct ^{4}He(π^+,pnp) cross section has never been measured. In any event, we cannot expect the cross section to be large enough to explain the large ratio observed at PSI. Some higher-order processes and enhancement due to the soft FSI must be added to the SMFP model. the yield ratio was much smaller for the TRIUMF data. The disagreement is difficult to explain from the incident pion energy or the energy threshold of detectors. A possible reason is that the counter configuration of TRIUMF is more convenient for the two-step processes as described above.

The MC calculation for the SMFP model could reproduce fairly well the existing double- and triple-coincidence data of pion absorption on ^{3}He and ^{4}He, using only well-known reaction mechanisms and nuclear data. Moreover, the shoulder at the larger angle side of the 2NA peak in the ^{3}He(π^+,pp) angular distribution and the shoulder at 110 MeV in the coincident proton energy spectrum could be reproduced uniquely by taking into account the ISI of incident pions. The energy spectrum of coincident proton for the ^{3}He(π^+,pp) reaction could be reproduced at an angular region far from 2NA, except for the low proton energy region. Three possible reasons for the discrepancy may be considered. The first is the interference between processes, which may induce strong deformation in energy spectrum, as demonstrated by Lee [8] in the three-body rescattering calculation. The second is the reliability on the energy scale with the long plastic scintillator detector. The peak energy corresponding to 2NA is shifted to lower energy from calculated value. The last is the neglect of more complex processes including the emission of quasibound pn or pp, higher-order multiple scattering and the genuine many-nucleon absorption process. The differential cross section for the triple-coincidence ^{4}He(π^+,ppp) could be reproduced very well at the lower-momentum region of the spectator nucleon. Present SMFP model can also reproduce the differential cross section for the reaction ^{2}H(p,pp)n at 508 MeV [22] for neutron recoil momenta larger than 200 MeV/c, where hard FSI plays an important role [23].

In conclusion, most available data for pion absorption on He could be explained by the SMFP model, and no active reason could be found for including the genuine three-nucleon absorption mechanism, except for the low-energy part of the coincident proton energy spectrum. As the triple-coincidence measurement at PSI and TRIUMF concluded that the three-nuelcon absorption cross section is less than 15% of the total absorption cross section at 120 and 165 MeV for ^{4}He which has high nucleon density, it seems difficult to consider the process dominant in heavier nuclei. On the contrary, the role of the multistep processes increase with target mass. It is absolutely necessary to study new absorption mechanism in a few-nucleon system; however, the present study shows that it is important to measure double- and triple-coincidence yields at a counter configuration far from two-step processes, using counters with better angular and energy resolution.

[1] M. A. Moinester *et al.*, Phys. Rev. Lett. **52**, 1203 (1984).
[2] P. Weber *et al.*, Nucl. Phys. **A501**, 765 (1989).
[3] M. Steinacher *et al*, Nucl. Phys. **A517**, 413 (1990).
[4] H. Yokota *et al.*, Phys. Rev. Lett. **57**, 807 (1986).
[5] H. Yokota *et al.*, Phys. Rev. C **39**, 2090 (1989).
[6] K. Masutani and K. Yazaki, Phys. Lett. **104B**, 1 (1981).
[7] V. Girija and D. S. Koltun, Phys. Rev. Lett. **52**, 1397 (1984).
[8] T.-S. H. Lee, Phys. Rev. C **31**, 2163 (1985).
[9] H. W. Bertini, Phys. Rev. C **6**, 631 (1972).
[10] H. Yokota *et al.*, Phys. Rev. Lett. **58**, 191 (1987).
[11] H. Yokota *et al.*, Phys. Rev. C **40**, 270 (1989).
[12] G. Backenstoss *et al.*, Phys. Rev. Lett. **55**, 2782 (1985).
[13] G. Backenstoss *et al.*, Phys. Lett. B **222**, 7 (1989).
[14] G. Backenstoss *et al.*, Phys. Rev. Lett. **61**, 923 (1988).
[15] M. L. Goldberger and K. M. Watson, *Collision Theory* (Wiley, New York, 1964), p. 760.
[16] J. G. Rogers and D. P. Saylor, Phys. Rev. C **6**, 734 (1972).
[17] R. D. Haracz and T. K. Lim, Phys. Rev. C **10**, 431 (1974).
[18] C. Marchand *et al.*, Phys. Rev. Lett. **60**, 1703 (1988).
[19] R. Ent, H. P. Blok, J. F. J. van den Brand, H. J. Bulten, E. Jans, L. Lapikas, and H. Morita, Phys. Rev. Lett. **67**, 18 (1991).
[20] P. Weber *et al.*, Phys. Lett. B **230**, 31 (1989).
[21] F. Adimi *et al.*, Phys. Rev. C **45**, 2589 (1992).
[22] M. B. Epstein *et al.*, Phys. Rev. C **42**, 510 (1990).
[23] H. Yokota (unpublished).